

## Deconvolution of “Drizzled” and Rotated HST/WFPC2 Images: Faint-object Photometry in Crowded Fields

Raymond Butler, Aaron Golden, Andrew Shearer

*Department of Information Technology, National University of Ireland  
Galway, University Road, Galway, Ireland*

**Abstract.** We have further adapted our deconvolution-based HST/WFPC2 reduction techniques, which our simulations have shown to be very effective in crowded fields (Butler 2000), to take advantage of the extra resolution afforded by “dithered” observations. This appears to be the first attempt at *non-linear* restorations of data which had already been sub-sampled and combined in a *linear* manner using the *STSDAS/drizzle* software, thus attaining a net subsampling factor of  $4\times 4$ . The motivation was a search for the optical counterpart of the millisecond pulsar PSR B1821-24 in the globular cluster M28; the technique is illustrated by our photometric search for candidates in the radio-derived error circle, in archival HST/WFPC2 images in both the F555W & F814W bands of the core field of M28.

### 1. Introduction: HST/WFPC2 Photometry Challenges

Although difficult, ground-based photometry of faint objects in crowded fields does not really compare with crowded-field photometry with a space-based telescope/camera, e.g., HST/WFPC2, which features an undersampled and spatially varying point-spread function (PSF), with high-frequency structure in the PSF “wings”. These factors, plus the sheer number of stars which may require measurement as a single group, cause a variety of practical problems for star detection and photometry, which were detailed in Butler (2000).

### 2. An Optical Counterpart to PSR B1821-24 in M28?

In this paper we examine solutions to the above issues by taking an example, the post-core-collapse globular cluster M28/NGC 6626. We obtained two sets of archival HST/WFPC2 observations of M28 as follows: (1) 424 sec in F555W & 423 sec in F814W taken on 8/08/97 (P. I. Gebhardt); (2) 1128 sec in F555W & 1508 sec in F814W taken on 12/09/97 (P. I. Buonanno). Both datasets were taken in dithered mode, with steps of 3.666 pixels (epoch 1) or 2.745 pixels (epoch 2) in X and Y on the PC1 chip. There is a relative rotation of  $12^{\circ}.875$  between the two datasets. Finally, the cluster core is centred on the PC1 chip. There is an object of great interest to us in this core field. PSR B1821-24 is a millisecond radio pulsar (period  $P \sim 3$  ms; see e.g., Cognard et al. 1996) in M28. The fact that the magnetic field & spin coupling is of a similar magnitude

to that of the Crab pulsar in the vicinity of the light cylinder has suggested that the millisecond pulsar may well be an efficient nonthermal emitter. The confirmation by the ASCA satellite of a strong synchrotron dominated hard X-ray pulse fraction (Saito et al. 1997) encourages such a viewpoint. Using phenomenological models of pulsar magnetospheric emission (Pacini & Salvati 1987; Shearer & Golden 2000), the predicted optical luminosity is estimated at  $V_0 \sim 21.5\text{--}23.5$ , which would be reduced to an observable  $V \sim 23\text{--}25$  by the interstellar extinction towards M28 of  $A_V \sim 1.4$  mag (Davidge et al. 1996). This would yield the first optical millisecond pulsar, indeed the first optical pulsar in a globular cluster or any such old stellar population. But PSR B1821-24 lies only  $\sim 12''$  from the center of M28, so a targeted high-resolution search of the entire radio error circle to  $V \sim 25$  is a challenge—even with HST.

### 3. Image Processing & Photometry

There are many advantages to “drizzling” HST/WFPC2 images (Fruchter & Hook 1997). It genuinely restores some of the resolution lost to undersampling; it resamples onto a regular astrometric grid, with the option of subsampling the images by  $2 \times 2$ ; and it is a *linear* reconstruction method, so the resulting stellar profile shapes are not dependent on signal/noise and the noise statistics remain “physical.” This makes it an excellent starting point for our *non-linear* subsampled MEM (Maximum Entropy Method) deconvolution approach to star detection and crowded-field photometry on HST/WFPC2 images. The latter also has many advantages. Star detection is improved because the actual HST PSF shape, in all its complexity, is used (via deconvolution) to “Gaussianise” the PSF while also better separating the stars from each other. Photometry is also slightly improved; our simulations (Butler 2000, Butler & Shearer 2001) have shown that aperture photometry on the subsampled MEM-deconvolved images is superior to all of the following conventional reductions of the original data: aperture photometry, profile-fitting photometry, and the hybrid method of aperture photometry on neighbour-subtracted images (e.g., Yanny et al. 1994).

We combined both these processes as follows. The images were “drizzled” and cleaned in the normal way, subsampling by a factor of 2. A series of “dithered” synthetic PSF grids were also “drizzled:” the “stars” were a uniformly distributed  $6 \times 6$  grid of normal-sampled Tiny Tim (Krist & Hook 1996) synthetic PSFs for each WFPC2 chip & filter combination, computed at high spatial subsampling, shifted to reproduce the dither offset, rebinned to normal sampling and convolved with the pixel scattering kernel. Instances of the PSF were obtained for deconvolution, at any desired position and with a further  $2 \times$  subsampling factor, after combining them using a quadratically variable DAOPHOT-II (Stetson 1994) model. Highly overlapping subimages of the field were deconvolved with these PSFs; the deconvolved subimages were reassembled into a whole sharpened, subsampled image for each filter and epoch. The four deconvolved images (F555W and F814W each at two epochs) were combined with a moderate rejection threshold: this eliminated nearly all artifacts, because (a) the radial structure of the PSF changed (due to the waveband dependence of the PSF shape), and (b) the position-angle of the PSF structure on the sky changed (due to the rotation changes). We used this deep, clean, sharp

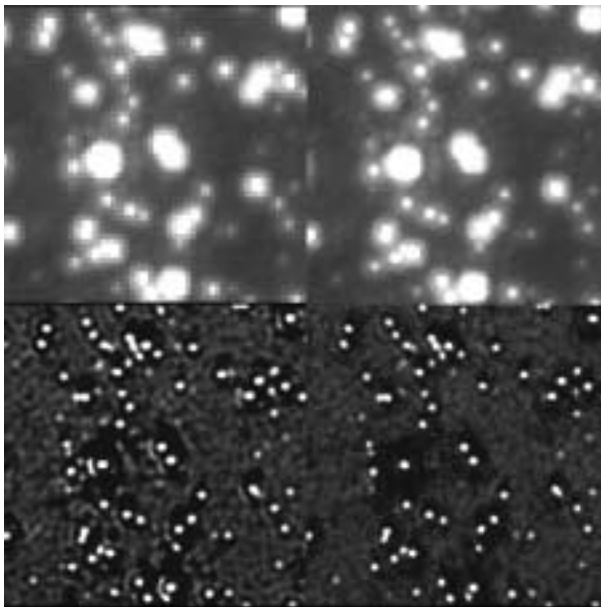


Figure 1. Section of HST/WFPC2 image of the globular cluster M28,  $2''.91$  on a side (corresponding to 64 PC1-chip pixels). Clockwise from upper left: Original (F814W epoch 2), Drizzled (F814W epoch 2), Deconvolved (F814W epoch 2), and Coadded after Deconvolution (F814W & F555W, both epochs: used for star detection).

coadded image for star detection. We then performed PSF-fitting photometry on the original “drizzled” images with this starlist and the existing PSF models. All but  $\approx 120$  selected bright “PSF stars” were subtracted from each image and a spatially-varying empirical PSF model was computed. The deconvolution & photometry steps were repeated with the refined PSFs. The final photometry was aperture photometry on these improved deconvolved images—both fast and accurate.

#### 4. Results & Conclusions

Examination of the radio-derived error circle yielded several potential candidates, down to a magnitude of  $V_0 \sim 23.0$ ; but both in the context of the CMD of M28, and with regard to phenomenological models of pulsar magnetospheric emission, none of them exhibited emission expected from a magnetospherically active pulsar (Golden, Butler, & Shearer 2000). The *key point*, however, is that the starlist in the field of PSR B1821-24, obtained via our drizzling plus deconvolution technique, is more reliable than that obtained by Sutaria (2000) with a subset of this same data (i.e., F555W epoch 2), which appears to be contaminated with several faint spurious detections. We therefore believe that deconvolution of “drizzled” and rotated images ( $\geq 2$  spacecraft roll angles) is the optimal way to detect and measure faint objects in crowded fields imaged with HST, and we recommend such an observing strategy.

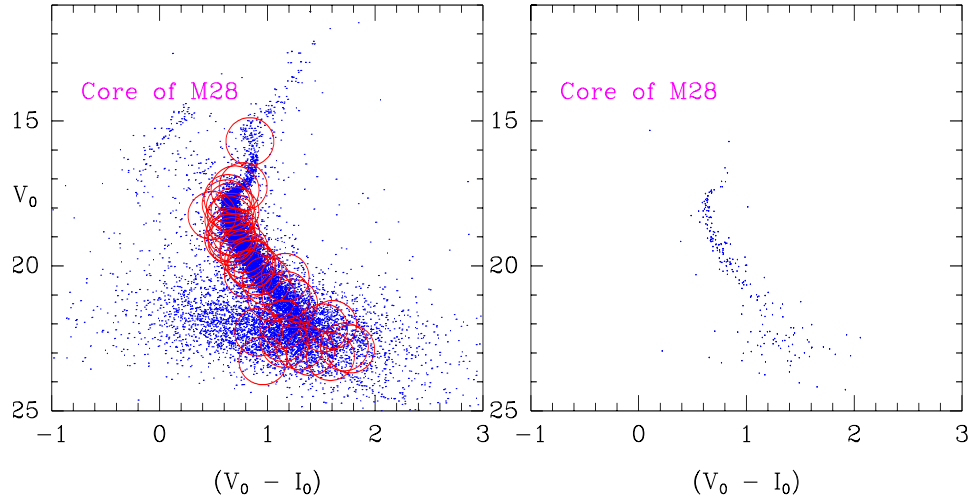


Figure 2. Left: The M28 CMD - de-extincted and re-reddened - for all stars on the PC1 chip of HST/WFPC2. The stars within the radio-derived error circle of PSR B1821-24 are shown by large circles. Right: The M28 CMD for the  $4''.55 \times 4''.55$  region centered on PSR B1821-24.

**Acknowledgments.** We gratefully acknowledge financial support from Enterprise Ireland (Basic Research Programme) and the European Commission (TMR Fellowship ERBFMBICT972185 funded much of this work, performed by RB at the University of Edinburgh, UK [TMR host: Prof. Douglas Hoggie]). This work was based upon HST data obtained from the ST-ECF (ESO) archive.

## References

- Butler, R. F. 2000, in ASP Conf. Ser., Vol. 216, *Astronomical Data Analysis Software and Systems IX*, ed. N. Manset, C. Veillet, & D. Crabtree (San Francisco: ASP), 595
- Butler, R. F. & Shearer, A. 2001, in preparation for PASP
- Cognard, I., et al. 1996, *A&A*, 311, 179
- Davidge, T. J. 1996, *ApJ*, 468, 641
- Fruchter, A. & Hook, R. N. 1997, *Proc. SPIE*, 3164, 120
- Golden, A., Butler, R. F., & Shearer, A. 2000, submitted to *A&A*
- Krist, J. & Hook, R. 1996, *Tiny Tim User's Manual, V4.2* (Baltimore: STScI)
- Pacini, F. & Salvati, M. 1987, *ApJ*, 321, 447
- Saito, Y., et al. 1996, *ApJ*, 477, L37
- Shearer, A. & Golden, A. 2000, accepted for publication in *ApJ*
- Stetson, P. B. 1994, *PASP*, 106, 250
- Sutaria, F. K. 2000, in *Pulsar Astronomy—2000 and Beyond*, *Proc. IAU Coll. 177*, ed. M. Kramer, N. Wex, N. Wielebinski (San Francisco: ASP), 313
- Yanny, B., Guhathakurta, P., Schneider, D., & Bahcall, J. 1994, *ApJ*, 435, L59